

Properties of the CdTe/InSb interface studied by optical and surface analytical techniques

Z. C. Feng^{*,1}, S. Y. Hung¹, and A. T. S. Wee²

¹ Graduate Institute of Electro-Optical Engineering & Department of Electrical Engineering, National Taiwan University, Taipei, 106-17 Taiwan, ROC

² Department of Physics, National University of Singapore, Singapore 119260

Received 5 September 2005, revised 2 June 2006, accepted 2 June 2006

Published online 13 July 2006

PACS 68.35.Dv, 68.49.Sf, 78.55.Cr, 79.60.Bm, 81.15.Hi

Indium interdiffusion in MBE-grown CdTe/InSb heterostructures was studied by optical and surface techniques of photoluminescence (PL), X-ray photoelectron spectroscopy (XPS) and secondary ion mass spectrometry (SIMS). A correlation between the two types of investigations is established.

© 2006 WILEY-VCH Verlag GmbH & Co. KGaA, Weinheim

1 Introduction

CdTe is an important material for radiation detectors and photovoltaic (PV) solar cells [1], with various active research activities in recent two decades [1–18]. CdTe/InSb is a significant system because of the very close lattice mismatch ($\Delta a/a \sim 5 \times 10^{-4}$) between them [6, 18], and therefore, the dissimilar heteroepitaxy between II–VI and III–V compounds, such as CdTe on InSb or InSb on CdTe, is very attractive for applications in optoelectronics [6, 9–11, 13, 14, 16–18]. We have recently performed a series of investigations on CdTe/InSb heterostructures grown by molecular beam epitaxy (MBE) [9, 11, 16–18]. The crystalline perfection and optical/structural properties of CdTe thin films on InSb were greatly affected by the InSb substrate growth temperature, T_s , and other growth conditions. It has been reported [5, 6, 10, 13] that In diffuses easily across the CdTe/InSb interface and modifies the optical and electronic properties of epitaxial CdTe. In this work, we present a combined study of optical and surface science analyses on the indium interdiffusion in MBE-grown CdTe/InSb heterostructures.

2 Experimental

The CdTe films were grown in an MBE machine on (001) InSb substrates which were polished on both sides, ion beam cleaned and subsequently annealed at ~ 200 °C prior to MBE growth. Two typical samples involved in this study, No. 248 and 217, were grown at the same growth rate of 0.70 $\mu\text{m/hr}$ to a film thickness of about 1.4 μm , but at different substrate growth temperatures, T_s , of 200 °C for No. 248 and 265 °C for No. 217. PL measurements were performed at 2 K, excited by the Ar^+ -514.5 nm line with 4.3 mW focused at 200 μm spot, and detected by a PL system with a 0.75 m spectrometer, a cooled GaAs cathode photomultiplier and a lock-in amplifier under computer control.

X-ray photoelectron spectroscopy (XPS) experiments were performed in a VG ESCALAB MkII using a Mg K_α X-ray source (1253.6 eV, 120 W) at a constant analyzer pass energy of 20 eV. The SIMS depth profiles were taken in a VG SIMSLAB connected to the ESCALAB via a preparation chamber using a

* Corresponding author: e-mail: zcfeng@ee.cc.ntu.edu.tw, Phone: +886 2 3366 3543, Fax: +886 2 2367 7467

9 keV 20 nA Ar⁺ beam produced from a differentially pumped VG DP50B douplasmatron ion gun, detected by a VG MM12-12 quadrupole mass spectrometer (0–800 amu).

3 Results

3.1 Low-temperature photoluminescence

Figure 1 shows 2 K PL spectra of (a) the $T_s = 200$ °C sample (No. 248) and (b) the $T_s = 265$ °C one (No. 217). The former shows the free exciton transition $X_{n=1}$ at 1.596 eV, the upper branch of free exciton-polariton X_{UP} at 1.599 eV, the acceptor bound exciton A_α at 1.591 eV with its one longitudinal optical (LO) replica A_α -1LO, a donor-acceptor-pair (DAP) transition P at 1.548 eV with its 1LO phonon replica P_1 , and deep level recombination bands of B at 1.499 eV and C at 1.495 eV as well as their corresponding phonon replicas, $B_1, B_2, B_3, C_1,$ and C_2 [18]. The latter with higher T_s exhibits PL spectra with only A_α similar to the sample with lower T_s , and more defects-related features, such as D_μ at 1.593 eV which is associated with donor-like structural defects or impurity-defect complexes, E and F bands which were assigned to excitons bound to acceptor-like structural defects or defect-impurity complexes, and defect-related 1.44 eV broadband [1, 17].

3.2 Secondary ion mass spectrometry (SIMS)

Figure 2 displays the comparative SIMS depth profiles of these two samples. The In⁺ profiles show that the In concentration in the entire CdTe layer is higher for the $T_s = 265$ °C sample than that for the $T_s = 200$ °C sample, even at the surface. Furthermore, the In⁺ profile is consistent with In diffusing outwards from the InSb substrate and accumulating at the CdTe surface. Other Cd⁺, Te⁺ and Sb⁺ profiles are quite similar from two samples with only Sb⁺ shown in Fig. 2, for a comparison with In⁺.

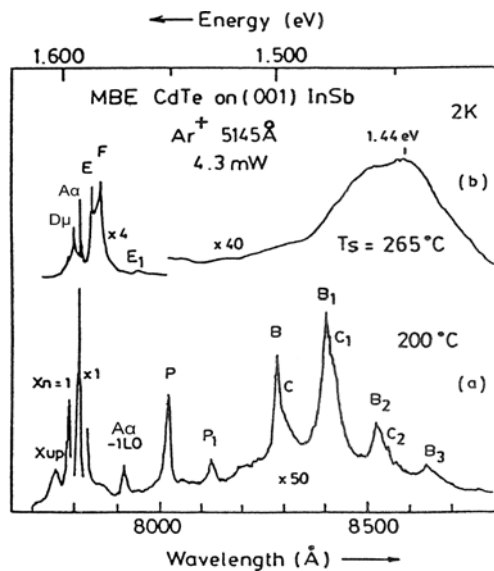


Fig. 1 2 K PL spectra of MBE-grown CdTe/InSb with (a) $T_s = 200$ °C (No. 248) and (b) $T_s = 265$ °C (No. 217).

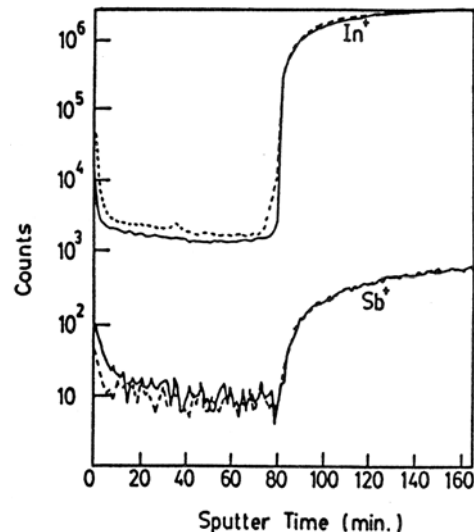


Fig. 2 SIMS depth profiles showing In⁺ and Sb⁺ signals of MBE-grown CdTe/InSb heterostructures at $T_s = 200$ °C (solid lines) and $T_s = 265$ °C (dashed lines).

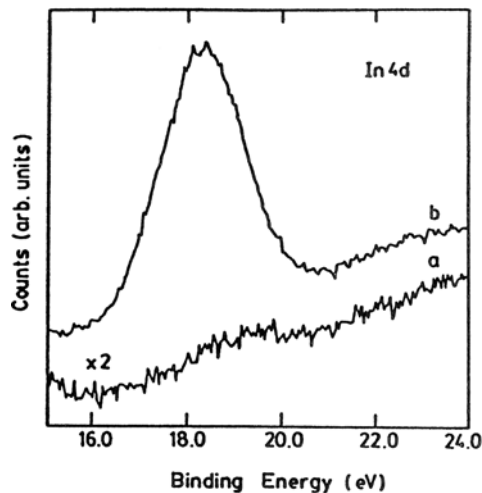


Fig. 3 XPS In 4d signals, as-received, of MBE-grown CdTe/InSb at (a) $T_s = 200^\circ\text{C}$ and (b) $T_s = 265^\circ\text{C}$.

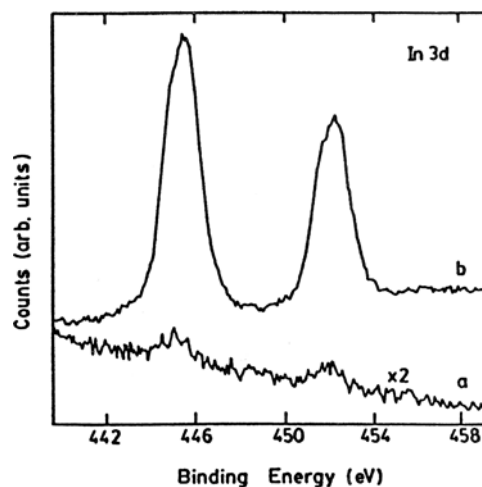


Fig. 4 XPS In 3d signals, after light Ar^+ sputtering, of MBE-grown CdTe/InSb at (a) $T_s = 200^\circ\text{C}$ and (b) $T_s = 265^\circ\text{C}$.

3.3 X-ray photoelectron spectroscopy (XPS)

Figure 3 shows the comparative XPS In 4d energy spectra, for these two as-received samples, while Fig. 4 shows their XPS In 3d spectra after light Ar^+ sputtering to remove any surface contaminants. Strong In signals appear from the $T_s = 265^\circ\text{C}$ sample in both figures while the signals are significantly weaker for $T_s = 200^\circ\text{C}$ sample. Note that XPS probes only the surface region to a depth of about 5 nm. Since the as-received and sputtered In 4d and 3d XPS spectra are virtually unchanged for both samples, we conclude that these In signals are not due to subsequent surface contamination.

4 Discussion

From the present study, the following observations are obtained:

(1) The surface analytical techniques reveal In interdiffusion directly. The SIMS depth profile and the XPS In 3d and 4d spectra indicate that the In concentration in the CdTe film grown at high T_s is significantly higher than that at low T_s , and this can be attributed to indium interdiffusion from the InSb substrate. Higher substrate growth temperatures enhances In interdiffusion across the CdTe/InSb interface, leading to a higher indium concentration in the $T_s = 265^\circ\text{C}$ sample.

(2) PL spectra from the two T_s samples are quite different. The low T_s sample possesses strong free and acceptor-bound excitons, and relatively weaker and sharper emissions in the deep level range of 1.4–1.5 eV, characteristic of high quality single crystalline CdTe [18]. The high T_s sample has a dull FE feature only, a stronger donor-bound exciton like feature associated with structural defects, strong defect-related E and F lines and a deep 1.44 eV broad band [18]. Previous TEM observations had shown that high T_s CdTe films contain a high density of dislocations [17]. The above PL features from the high T_s CdTe film have been associated with structural defects or impurity-defect complexes [17, 18]. The present study shows that the impurity involved in these complexes should be mainly indium.

CdTe is well lattice matched with InSb. The lattice constant for CdTe, $a(\text{CdTe})$, is 0.6486 nm or 0.6482 nm at room temperature (RT) [14]. The $a(\text{InSb})$ lattice constant is 0.6479 nm [18]. The difference between them is 0.1% or 0.04% with the lattice constant of $a(\text{CdTe})$ being slightly higher than that of $a(\text{InSb})$. The linear thermal expansion coefficient α of InSb is about $5.5 \times 10^{-6}/\text{K}$ between 10°C and 60°C , while $\alpha(\text{CdTe}) = (4.70\text{--}4.90) \times 10^{-6}/\text{K}$ at 283 K which is lower than the value of $\alpha(\text{InSb})$.

We had previously varied T_s between 170 °C and 285 °C and obtained an optimum T_s of 185 °C. The CdTe films grown at this T_s and below 200 °C show high crystalline perfection [18]. Indeed, PL and structural features of CdTe films grown under 185–200 °C are quite similar. Growth at higher T_s within this range is better to avoid the Te-droplets. Their cross-sectional TEM (XTEM) images across the CdTe/InSb interface are very clean and without obvious dislocations. However, the CdTe/InSb interface of $T_s > 250$ °C samples were filled with numerous dislocations, stacking faults and micro-cracks, the density of which increased with increasing T_s between 225 °C and 285 °C.

To explain the above features, we may assume that there would exist an exact lattice match between CdTe and InSb at 185 °C (or below 200 °C) and that $a(\text{CdTe}) > a(\text{InSb})$ as $T_s < 185$ °C and $a(\text{CdTe}) < a(\text{InSb})$ as $T_s > 185$ °C or 200 °C. This difference in lattice constants increases beyond 225 °C. As we grow CdTe on InSb at a higher T_s , the larger lattice mismatch would lead to dislocation lines into CdTe and the development of these dislocation lines. A large amount of In leads to the strong signals in the XPS spectra and SIMS profiles, and also to the strong In- and defect-related PL emissions from the top CdTe layers.

5 Conclusion

In conclusion, the interface properties of CdTe/InSb grown by molecular beam epitaxy (MBE) and the In interdiffusion were studied by optical and surface techniques of photoluminescence (PL), X-ray Photoelectron Spectroscopy (XPS) and Secondary Ion Mass Spectrometry (SIMS). The In interdiffusion has been revealed directly by SIMS depth profile and XPS In 3d and 4d spectra, indicating that the In concentration in CdTe film grown with high substrate growth temperature T_s is much higher than that with low T_s . Higher T_s enhanced the In interdiffusion across the CdTe/InSb interface, leading to more indiums detected. These are correlated to the PL spectra from two T_s samples which are quite different. The low T_s one possesses strong free and acceptor-bound excitons, relatively weaker and sharp emissions in the deep level range of 1.4–1.5 eV, characteristic of high quality of single crystalline CdTe. The high T_s one has dull FE feature only and strong defect-related E and F lines and deep 1.44 eV broad band. It predicts that there would exist an exact lattice match between CdTe and InSb at the optimum T_s of 185 °C and that $a(\text{CdTe}) > a(\text{InSb})$ as $T < 185$ °C and $a(\text{CdTe}) < a(\text{InSb})$ as $T > 185$ or 200 °C. At higher T_s , the bigger lattice mismatch would lead to dislocations and In will diffuse more efficiently along these dislocation lines from InSb substrate into CdTe layer. The big amount of In leads to the strong signals of XPS spectra and SIMS profiles, and also to the strong In- and defect-related PL features. Optimizing T_s and other growth conditions are efficient to depress the In interdiffusion during the II–VI/III–V growth.

Acknowledgements We would like to thank Profs. W. J. Choyke and R. F. C. Farrow for help in this work. The work at National Taiwan University was supported by funds from National Science Council of Republic of China, NSC 93-2218-E-002-011, 93-2215-E-002-035 and 94-2215-E-002-019.

References

- [1] C. R. Corwine, J. R. Sites, T. A. Gessert, W. K. Metzger, P. Dippo, Jingbo Li, A. Duda, and G. Teeter, *Appl. Phys. Lett.* **86**, 221909 (2005).
- [2] D. Shvydka, J. P. Rakotoniaina, and O. Breitenstein, *Appl. Phys. Lett.* **84**, 729 (2004).
- [3] Y. Yan, M. M. Al-Jassim, and K. M. Jones, *J. Appl. Phys.* **94**, 2976 (2003).
- [4] M. J. Romero, D. S. Albin, M. M. Al-Jassim, X. Wu, H. R. Moutinho, and R. G. Dhere, *Appl. Phys. Lett.* **81**, 2962 (2002).
- [5] M. J. Soares, M. C. do Carmo, *Proc. SPIE* **4469**, 57 (2001).
- [6] J. Huerta-Ruelas, M. Lopez-Lopez, and O. Zelaya-Angel, *Jpn. J. Appl. Phys.* **39**, 1701 (2000).
- [7] Y.-H. Kim, S.-Y. An, J.-Y. Lee, I. Kim, K.-N. Oh, S.-U. Kim, M.-J. Park, and T.-S. Lee, *J. Appl. Phys.* **85**, 7370 (1999).
- [8] C. Heske, U. Winkler, H. Neureiter, M. Sokolowski, R. Fink, E. Umbach, Ch. Jung, and P. R. Bressler, *Appl. Phys. Lett.* **70**, 1022 (1997).

- [9] Z. C. Feng, H. Gong, W. J. Choyke, N. J. Doyle, and R. F. C. Farrow, *J. Mater. Sci., Mater. Electron.* **7**, 23 (1996).
- [10] D. Drew, J. Sahm, W. Richter, and D. R. T. Zahn, *J. Appl. Phys.* **78**, 4060 (1995).
- [11] A. T. S. Wee, Z. C. Feng, H. H. Hgn, K. L. Tan, R. F. C. Farrow, and W. J. Choyke, *J. Phys.: Condens. Matter* **7**, 4359 (1995).
- [12] S. Tatarenko, F. Bassani, J. C. Klein, K. Saminadayar, J. Cibert, and V. H. Etgens, *J. Vac. Sci. Technol. A* **12**(1), 140 (1994).
- [13] M. S. Boley, R. J. Thomas, M. Chandrasekhar, H. R. Chandrasekhar, A. K. Ramdas, M. Kobayashi, and R. L. Gunshor, *J. Appl. Phys.* **74**, 4136 (1993).
- [14] T. W. Kim, M. Jung, H. L. Park, H. K. Na, and J. S. Kim, *Appl. Phys. Lett.* **61**, 1101 (1992).
- [15] N. C. Giles, K. A. Bowers, R. L. Harper, Jr., S. Hwang, and J. F. Schetzina, *J. Cryst. Growth* **101**, 67 (1990).
- [16] Z. C. Feng, S. Perkowitz, J. M. Wrobel, and J. J. Dubowski, *Phys. Rev. B* **39**, 12997 (1989).
- [17] Z. C. Feng, M. G. Burke, and W. J. Choyke, *Appl. Phys. Lett.* **53**, 128 (1988).
- [18] Z. C. Feng, A. Mascarenhas, and W. J. Choyke, *J. Lumin.* **35**, 329 (1986).